Color Glass Condensate in Brane Models or Don't Ultra High Energy Cosmic Rays Probe $10^{15}eV$ Scale ?

Houri Ziaeepour
Mullard Space Science Laboratory,
Holmbury St. Mary, Dorking, Surrey RH5 6NT, UK.
Email: hz@mssl.ucl.ac.uk

Abstract

In a previous work [1] we have studied propagation of relativistic particles in the bulk for some of the most popular brane models. Constraints have been put on the parameter space of these models by calculating the time delay due to propagation in the bulk of particles created during the interaction of Ultra High Energy Cosmic Rays (UHECRs) with protons in the terrestrial atmosphere. The question was however raised that probability of hard processes in which bulk modes can be produced is small and consequently, the tiny flux of UHECRs can not constrain brane models. Here we use Color Glass Condensate (CGC) model to show that effects of extra dimensions are visible not only in hard processes when the incoming photon/parton hits a massive Kaluza-Klein mode but also through the modification of soft/semi-hard parton distribution. At classical level, for an observer in the CM frame of UHECR and atmospheric hadrons, color charge sources are contracted to a thin sheet with a width inversely proportional to the energy of the ultra energetic cosmic ray hadron and consequently they can *see* an extra dimension with comparable size. Due to QCD interaction a short life swarm of partons is produced in front of the sheet and its partons can penetrate to the extra-dimension bulk. This reduces the effective density of partons on the brane or in a classical view creates a delay in the arrival of the most energetic particles if they are reflected back due to the warping of the bulk. In CGC approximation the density of swarm at different distances from the classical sheet can be related and therefore it is possible (at least formally) to determine the relative fraction of partons in the bulk and on the brane at different scales. Results of this work are also relevant to the test of brane models in hadron colliders like LHC.

1 Introduction

The concept of string compactification with non-compact [2] and warped spaces [3] [4] has been introduced in the 90's and since then it has been considered as one of the favorite candidates for solving the hierarchy problem in Particle Physics. Naturally also, a large number of works have been devoted to observe the effects of a macroscopic extra-dimension in high energy particle colliders [8] [9], short distance gravity experiments [5] and in cosmological contest [6] [10] [11] - just to cite some of the first works on these subjects.

In [1] (from now on "Paper I") we have used the time coherence of high energy air showers produced in the terrestrial atmosphere by Ultra high Energy Cosmic Rays (UHECRs) to constrain brane models. Assuming that the primaries are a single elementary particle (most probably proton or anti-proton), these events are the most energetic particle collision available to us at present. The energy scale of these events is $\sim 10^{15}eV$ roughly 3 orders of magnitude higher than available energies even in near future accelerators like LHC. If the fundamental scale of gravity is $10^{12}eV \lesssim M_5 \lesssim 10^{15}eV$, it must leave a signature on the high energy air-showers. Some authors have studied the possibility of production of microscopic black holes during this process [12] and have constrained low-scale gravity models with extra-dimension. Delay in the arrival time of most energetic particles is another expected effects if extra-dimensions are accessible to primary particles produced during the interaction of UHECR primaries with nucleons in the atmosphere. We have studied this possibility in Paper I and we continue the investigation here by studying the details of QCD interactions in presence of one extra dimension.

In Paper I we treated particles as free and by solving their wave equation we showed that in 2-brane models KK-modes have a roughly continuous spectra beginning from their 5-dim mass. We also determined relative coupling (branching ratio) for bulk and brane modes and thereby showed that the probability of KK-mode production is much higher than the zero-modes. Based on this knowledge we then studied the classical propagation of these particles - assumed to be relativistic - and we constrained a number of brane models. Propagation method has been also extensively used for studying the propagation in the bulk as an alternative to inflation [7] in the early universe.

This procedure however does not deal with details of KK-mode production, and the idea of using time coherence of high energy air-showers for testing brane models has been questioned based on the fact that cross-section of soft/semi-hard events - what is called small-x events - is much higher than events with significant transverse momentum permitting the production of heavy particles, presumably related to high energy scale physics (heavy KK-modes, GUT particles, etc.) [6]. Thereby, it is claimed that UHECRs do not probe $\sim 10^{15} eV$ scale, except probably by gravitational effects.

In the present work we use recent development in modeling small-x processes in hadron-hadron or Deep Inelastic Scattering (DIS) and their relation to higher x_b's[1] to calculate the distribution of partons - mainly gluons - in the bulk and on the branes. Before discussing the details of parton production we first highlight some of differences between observables in high energy colliders and in air-shower detectors. We also briefly review the issue of confinement of vector fields like gluons on the branes and their KK-mode's mass spectrum.

There is an essential difference between observables in colliders and in the air-showers. In the former case only particles with a transverse momentum greater than a minimum value which depends on the detector hole size are detectable and the remnants of the colliding beams which include most energetic particles are not visible. In contrast, in an air-shower it is *apriori* possible to detect all the particles specially the most energetic ones and there is no discrimination between semi-hard and high energy remnants and consequently, one is not restricted to see only high transverse momentum part of the collision[2].

Apriori the incident parton can be traced back to the point where it has $\sim 1/3$ of hadron momentum. At this scale if there is an extra space-time dimension, it contributes to the available parameter space of the transverse momentum. It is also true for the rest of the hadron bag which does not participate in the hard interaction. Giving the fact that the average initial transverse momentum of the partons is at least $\sim 200 MeV$, if they are ejected to the bulk - in a classical view of the process - they have enough energy to spend significant time there before being reflected back to the brane by the space bending.

On other hand, observation of small-x processes in HERA and Tevatron is not consistent with completely collinear radiation of partons before the (semi)hard reactions. The approximate angular ordering which has been observed in the Deep Inelastic Scattering (DIS)(see [26] for review of the observations and their phenomenology) is the evidence that most of particles with low transverse momentum (or more exactly the partons from which they are produced) have been emitted from the incoming hadrons very early i.e. at very short distance from emitting color charges (more details in next sections). At these short distance scales if higher dimension(s) are open to the physical processes on the brane, the emission to the bulk can influence the total number of particles produced on the brane at longer distance scales i.e. in hard or semi-hard interactions. We believe that this phenomenon was ignored by authors of ref. [6]. In addition, it is well known that in the warped brane models - the only type we consider in the present work - the spectrum of KK-modes is very close to a continuum beginning from m_5 the 5-dim mass with a slight gap between the zero-mode and higher KK modes [4] [13] [14] [15] [1]. The mass of KK-modes for all fields has the following general form

[1] When there is a risk of confusion between the coordinate x and Björken x, we distinguish the latter by subscript b.

[2] Here we implicitly assume that primaries are nucleons and interact with nucleons - hadron-hadron collision - or with electrons - Deep Inelastic Scattering in the atmosphere.

[16] [17] [20] [1]:

$$m_n \sim x_n \mu e^{-\mu L} \tag{1}$$

where m_n is the mass of nth KK-mode, $x_n \gtrsim 3$ for $n > 0$ and its exact value depends on the spin of the field. Parameter L is the effective size of the bulk. The gap between the zero-mode and higher modes is determined by the scale of the compactification μ. Warping of the extra-dimension - the conformal factor $e^{-\mu y}$ in the metric (4) is used to solve the problem of hierarchy between electroweak scale and 4-dim Planck scale and therefore in fine-tuned RS models:

$$\mu L \sim 36.8 - \log_{10}(M_5/TeV) \tag{2}$$

$$\mu = \frac{M_5^3}{M_{pl}^2} \tag{3}$$

If we consider μ as a free parameter and if we don't want to add another high energy scale to the model, the natural choice for compactification scale is M_5 the fundamental quantum gravity scale which must be close to Electroweak scale $\sim 1TeV$. It is easy to see that only if μ is of the order of the Planck energy, the first KK-modes will not be produced in the present colliders [16], otherwise KK-modes are light and apriori are easily produced in high energy collisions. In fact it has been shown that all the fields, specially spin-1 gauge fields [18] can propagate (tunnel) to a warped infinite or macroscopic bulk [19], unless some special setting prevents them [20] [15] [21]. In warped geometries fields in general are partially confined by gravitational force. However, as we will show in the next sections, quantum effects are much stronger and in presence of strong interactions like QCD, confinement by warping is not efficient.

A number of methods are suggested to localize gauge bosons on the visible brane. For example I. Oda [22] proposes to add a topological term to the Lagrangian. However, the induced gauge field on the brane is massive and it is not sure whether after taking into account radiative corrections their mass will be enough small to be compatible with observations. Recently it has been proved [23] that Einstein equation has a string-like defect solution which has a zero-mode for all fields of any spin. The space is not however warped but can have any number of infinite flat and/or compactified coordinates, and therefore the model can not solve the hierarchy problem. Moreover, it is not sure that the defect solution is stable and in any case as the metric is not warped, wave functions have a long extension in the bulk and are not really *localized*.

Another popular method for gauge boson localization is an induced gauge field kinetic term on the branes [13] [16]. The motivation is the necessity of adding such a term to the Lagrangian during renormalization. This method works only if charged fermions are confined to the brane. But it has been shown [14] that the universality of fermions' charge will be violated.

In summary it does not seem to be possible to confine all the SM fields on the brane even when the bulk metric is warped geometrically or just by a mild modification of the Lagrangian. The only way out if branes really exist is a symmetry which keeps at least most fields at energies lower than a threshold confined to the branes. This would be possible if branes are topological defects related to quantum gravity and created during a phase transition epoch in the early universe. If this broken symmetry prevents the production of KK-modes at low energies e.g. energies lower than fundamental gravity scale M_5, their direct production at present accelerator energies would be completely forbidden. For the same reason their effect on $Z_0/W^{\pm}$ width as well as gluon propagator would be extremely suppressed. If the fundamental scale of gravity in brane models is around EW scale, UHECR showers with Center of Mass (CM) energies larger than $\gtrsim 1TeV$ are expected to overcome restrictions (symmetry or else) which confine low energy events and extra-dimension(s) should highly influence the behavior of showers.

At high energies hadron-hadron collision and DIS are dominated by the physics of QCD cascade production of partons mainly gluons i.e. massless gauge vector bosons. For finding any evidence of an extra-dimension in these processes it is crucial to understand how the existence of an extra space dimension affects parton production on the visible brane. On the other hand, due to high density

of partons (mainly gluons) in the small-x regime, its study is very complicated and non perturbative effects should be taken into account. Since mid-1990s it has been shown [24] that a phenomenological treatment of the small-x regime known as McLerran-Venugopalan Color Glass Condensate (MVCGC) Model and its quantum extension [25] can explain observations by introducing a renormalization group like equation which gives the gluon distribution at each time ordering (transverse momentum) scale (see [27] for observational evidence of color gluon condensation). In fact, owing to this renormalization group equation, it is possible (at least formally) to obtain the distribution of partons at non-perturbative small-x regime from their distribution at higher energy scales where low-order perturbative QCD calculations are adequate. In this sense MVCGC is not just a model valid at small x_b but at all scales and the evidence for this claim is that at lowest order one can obtain BFKL approximation which is only valid at high energies - large x_b's - from MVCGC model.

Here we use this model to study the indirect effect of an extra-dimension on small-x processes. First we briefly review the basic ideas and principals of MVCGC model. Then we extend the zero-order (classical) MV model to a warped space-time and determine the distribution of gluons in the bulk and on the branes at high energies. Using the renormalization group equation in 4-dim we argue the effect of quantum corrections which lead to small-x events without detail calculation of relevant diagrams. Finally we apply the results of this model to a few brane models.

2 Color Glass Condensate in 4+1 Warped Space-Time

In this section we extend the formalism developed in [24] and [25] to 4+1 dimensional space-times with brane boundaries.
For an observer in the CM frame of the high energy incident hadrons (or lepton-hadron) they are contracted to a thin sheet perpendicular to the momentum direction. In McLerran-Venugopalan (MV) approximation it is assumed that color charge sources are concentrated only on these sheets. The origin of this charge is mostly valance quarks, but sea partons integrated up to a scale Λ^+ also contribute to the total charge. Soft partons (mostly gluons) make a swarm between these sheets and interact with the incident particles or their swarm. Although for very energetic collisions at all the interesting scales, QCD coupling between partons in the swarm and between the swarm and the color charge sheet(s) is less than 1 and therefore in the perturbative regime, it has been shown that due to the large density of partons, at very small x_b non-perturbative effects are very important [28]. In other word $\alpha_s \ln(1/x_b) > 1$ and perturbative QCD - BFKL evolution equation - is not sufficient.

2.1 Classical Solution

In McLerran-Venugopalan effective model for CGC the color sheet described above is considered as a classical source for gluon swarm. Because the lifetime of the swarm is much shorter than time variation of color charge density on the sheet at the scale of interest, the model can be roughly considered as static.

We consider a static Randall-Sundrum (RS) warped metric[3]:

$$ds^2 = \frac{R^2}{z^2}(\eta_{\mu\nu}dx^\mu dx^\nu - dz^2) = e^{-2\mu y}\eta_{\mu\nu}dx^\mu dx^\nu - dy^2 \quad (4)$$

$$z \equiv \frac{1}{\mu}e^{\mu y} \qquad \eta_{\mu\nu} = (1,-1,-1,-1) \quad (5)$$

Branes are considered to be at $z = R \equiv 1/\mu$ and $z = R' \equiv \frac{1}{\mu}e^{\mu L}$, where L is the distance between two

[3]We use upper case letters for 4+1 space, Greek letters for flat 3+1 metric and lower case letters for 3-space components.

branes. In light-cone coordinates:

$$x^+ = x^0 + x^3 \quad , \quad x^- = x^0 - x^3 \tag{6}$$

QCD interactions are modeled by an effective $SU(3)$ gauge field A^B of gluons. In Light Cone (LC) gauge $A^+ = 0$. For simplicity we neglect the color index except when its explicit indication is necessary. The classical dynamic equation is therefore:

$$[D_A, F^{AB}] = \delta^{B+}\rho(\vec{x}) \qquad \vec{x} \equiv (x^-, x^\perp, z) \tag{7}$$

$$D_A \equiv \partial_{;A} - igA^a_A T^a \tag{8}$$

The symbol ; means covariant derivation with respect to RS metric. Color charge ρ is + component of color current:

$$J^A(x) = \delta^{A+}\rho(x^-, x^\perp, z) \tag{9}$$

If fermions are confined to the visible brane $\rho \neq 0$ only for $z = R'$. However, we show later that this assumption is not consistent and is violated by a gauge transformation. We assume a universal coupling in the bulk and on the branes. Later we explain the effect of a kinetic term on the branes which is equivalent to an additional induced coupling.

The model defined by (7) and (8) is only valid at scale $\Lambda^+ = x_b P^+$ where P^+ is the energy of initial hadron and x_b is collinear momentum fraction of the parton (analogue to Björken x parameter). The scale Λ^+ indicates the maximum LC momentum of parton swarm and determines parton density at this scale. In classical MV model it is not possible to relate models at different scales. But when quantum corrections are added, it is possible to determine the evolution of parton density with scale Λ^+ and thereby relate gluon distribution at $x_b \to 0$ to $x_b \to 1$ and vice versa.

Conservation of color charges shows that in a general gauge the static charge gets a gauge rotation. The gauge-independent dynamic equation is therefore:

$$[D_A, F^{AB}](x) = \delta^{B+}\mathcal{W}(x^+, \vec{x})\rho(\vec{x})\mathcal{W}^\dagger(x^+, \vec{x}) \tag{10}$$

$$\mathcal{W}(x^+, \vec{x}) = T\exp\left\{ig\int_{x_0^+}^{x^+} d\eta^+ \frac{R^2}{z^2} A^-(\eta^+, \vec{x})\right\} \tag{11}$$

Time ordering operator T operates on $A^- \equiv A^-_a T^a$ and orders fields from right to left in increasing sequence of x^+. Physical quantities like 2-point correlation functions at classical (tree) level are obtained from solutions of (10) integrated over all possible $\rho(x)$ with probability distribution $W_{\Lambda^+}[\rho]$. From equations (10) and (11) one can easily conclude that even with $\rho(\vec{x}) = \rho(x^\perp)\delta(z)$, the gauge independent charge i.e. the right hand side of (10) and thereby F^{AB} depends on z.

In LC gauge equation (7) has a solution with $A^- = 0$ in addition to the LC gauge condition $A^+ = 0$ [28]. The solution for other components is:

$$\mathcal{A}_i = \frac{i}{g}\mathcal{U}(\vec{x})\partial_{;i}\mathcal{U}^\dagger(\vec{x}) \qquad i = x^\perp, z \tag{12}$$

with $\mathcal{U}$ an element of QCD $SU(3)$ group. In (12) $\mathcal{A}_i$ is the classical solution of the dynamic equation in LC gauge and should not be confused with A_i the general color field which includes also quantum corrections. This solution is not however very useful because the explicit dependence of $\mathcal{U}$ on ρ is not known. Nevertheless, it can be shown that in covariant gauge, equation (10) has a solution which is explicitly a functional of $\tilde{\rho}(\vec{x})$ the color charge density in covariant gauge [24]. Consider following gauge transformation:

$$\tilde{A}^B = \mathcal{U}^\dagger A^B \mathcal{U} + \frac{i}{g}\mathcal{U}^\dagger \partial^B_{;}\mathcal{U} \tag{13}$$

In LC gauge $A^+ = 0$ and $\tilde{A}^+$ has Kähler potential form:

$$\tilde{A}^+ = \frac{i}{g}\mathcal{U}^\dagger \partial^+_{;}\mathcal{U} \tag{14}$$

and equation (10) reduces to:

$$-\partial_{;i}\partial^i_{;}\tilde{A}^+ = \tilde{\rho}(\vec{x}) \qquad i = x^\perp, z \tag{15}$$

$$\tilde{\rho}(\vec{x}) \equiv \mathcal{U}^\dagger(\vec{x})\rho(\vec{x})\mathcal{U}(\vec{x}) \tag{16}$$

$\tilde{\rho}$ is color charge density in covariant gauge. Using (15), equation (14) can be inverted and:

$$\mathcal{U}(x^-, x^\perp, z) = P\exp\left\{ig\int_{x_0^-}^{x^-} d\eta^- \frac{R^2}{z^2}\tilde{A}^+(\eta^-, x^\perp, z)\right\} \tag{17}$$

where P orders $\tilde{A}^+ \equiv \tilde{A}^+_a T^a$ from right to left in increasing or decreasing order of x^- argument respectively for $x^- > x_0^-$ or $x^- < x_0^-$. The reason for formulating this model in both LC and covariant gauges is that the solution of (10) is simpler in covariant gauge, but physically interesting quantities like gluon distribution function have simpler description in LC gauge.

2.2 Gluon Propagator

For calculating the gluon distribution function (structure function) we need its propagator in the warped 4+1 space-time with MV approximation. This can be obtained from equation (15). Using the definition of covariant derivative, equation (15) expands to:

$$\partial_\perp^2\tilde{A}^+ + \partial_z^2\tilde{A}^+ - \frac{3}{z}\partial_z\tilde{A}^+ + \frac{3}{z^2}\tilde{A}^+ = \frac{R^2}{z^2}\tilde{\rho}(\vec{x}) \tag{18}$$

Note that $\tilde{A}^+$ dependence on x^- is not dynamical. This means that it should be fixed when boundary conditions are imposed. The rest of gauge freedom also will be fixed by boundary conditions and consequently, in the following we does not mention x^- explicitly. We define 2-dim Fourier transform of $\tilde{A}^+$ as:

$$\tilde{A}^+(k^\perp, z) = \int d^2x^\perp e^{ik_\perp x^\perp}\tilde{A}^+ \tag{19}$$

Applying this transformation to (18), the equation for $\Delta(z, z')$ the Green function of (18) can be obtained:

$$z^2\partial_z^2\Delta(z,z') - 3z\partial_z\Delta(z,z') + (3 - k_\perp^2 z^2)\Delta(z,z') = R^2\delta(z-z') \tag{20}$$

By redefining $\Delta(z, z')$ as:

$$\Delta(z,z') \equiv z^2\hat{\Delta}(z,z') \tag{21}$$

equation (20) is put in the following solvable form:

$$z^2\partial_z^2\hat{\Delta}(z,z') + z\partial_z\hat{\Delta}(z,z') + (k^2z^2 - 1)\hat{\Delta}(z,z') = R^2\delta(z-z') \tag{22}$$

with $k^2 = -k_\perp^2$. General solution of (22) is:

$$\hat{\Delta}(z,z') = C(z')J_1(kz) + D(z')N_1(kz) \tag{23}$$

where J_1 and N_1 are respectively Bessel function of first and second type. Integration constants $C(z')$ and $D(z')$ are determined by applying boundary conditions on the branes at $z = R$ and $z = R'$ as explained in detail in Paper I [1] with parameter $\nu = 0$ (see the definition of ν in Paper I). This results to following mass spectrum for KK-modes for large n:

$$m_n \approx R'^{-1}(\frac{3\pi}{4} \pm n\pi) \tag{24}$$

Therefore the coefficient x_n in (1) for lightest modes is ~ 2.36. Note that in this model the momentum of partons in the direction of the initial hadron i.e. $\Lambda^+ = x_b P^+$ appears only in the scale of the model or equivalently the color charge ρ.

It is worth to mention that the mass of all the gluon KK-modes in this model is real. This confirms the result obtained in [15] [1] for scalar fields. The spectrum begins from a massless zero-mode and there is a gap between zero-mode and higher modes proportional to $\mu' \equiv R'^{-1}$ which for all macroscopic bulk is very small. In fact for large $\mu L \gtrsim 30$, even for compactification scale $\mu \sim M_{pl}$, the mass of lightest KK-modes is much smaller than CM energy of UHECR interaction in the atmosphere and when the interaction scale $\Lambda^+ \gtrsim m_n$, KK-modes can be produced.

There is also a zero-mode with $k_\perp = 0$ with $\hat{\Delta}(z, z')$ satisfying:

$$z\partial_z(z\partial_z\hat{\Delta}(z,z')) - 1 = \frac{R^2}{z^2}\delta(z-z') \quad (25)$$

$$\hat{\Delta}(z,z') = C_0(z')z + D_0(z')z^{-1} \quad (26)$$

After applying the boundary conditions to (26), one finds that the integration constants $C_0(z')$ and $D_0(z')$ are in general non-trivial and therefore the zero-mode propagates to the bulk but its wave function exponentially decreases inside the bulk. This is a well known fact [18] and contrasts with scalar field case in which the Green function of the zero-mode is $\propto \delta(z-z')$ and consequently induces a discontinuity in the spectrum and separates zero-mode from higher KK-modes.

Propagation of gluon swarm to the bulk in CGC model has important implication for attempts to localize massless gauge bosons by adding an induced kinetic term on the branes. It has been shown [13] [16] that this term increases the coupling of the zero-mode to itself and if fermions are confined to the brane, the gauge vector field becomes quasi localized. Here it is easy to see that due to z dependence of $\tilde{A}^+$ and therefore $\mathcal{U}(\vec{x})$, according to (16), $\tilde{\rho}$ will depend on z even when ρ is confined to the brane. We will see later that because of the renormalization group equation which relates $W(\rho)$ the distribution of color charge density at each Λ^+ scale to other scales, ρ or $\tilde{\rho}$ gradually receives a z dependence, i.e. the color charge escape to the bulk even if initially - at large Λ^+ - it is concentrated on the brane. A more physical image of this process is obtained if one considers the transverse momentum ordering. At smaller x_b's partons have larger transverse momentum because they have lost their energy by QCD radiation which at the same time increases their transverse momentum. When an extra space dimension is available, with each radiation the transverse momentum of the out-going parton in the extra-dimension direction increases too.

2.3 Comment on the Observation of Massive KK-Modes

In Paper I it has been shown that the production probability of the massive KK-modes of a scalar field is higher than its zero-mode (Equation 2.27 in [1]). For gluons we can use the same formula with $k_0/\mu = 0$ and $\nu = 0$. Thus, the relative coupling and production probability of the zero-mode and n^{th} KK-mode is:

$$\frac{{g_0}^2}{{g_n}^2} \sim \left(\frac{m_n}{\mu}\right)^2 \quad (27)$$

$$P \sim \left(\frac{m_n}{\mu}\right)^4 \quad (28)$$

Due to warping factor and quasi-continuous spectrum of KK-modes the probability of production of bulk modes is much larger than the zero-mode. Moreover, because of the extension of the zero-mode's wave function into the bulk (in contrast to scalar and graviton cases), there is no significant observationally interesting difference between zero-mode and first KK-modes for gluon field.

If an additional coupling term is added to the Lagrangian, the mass spectrum of KK-modes is multiplied by the additional coupling. From (27) and (28) one can see that increasing the mass of KK-modes increases the coupling to the zero-mode on the branes [16]. However, according to calculation in [16], the effect of this term is only important when the compactification energy scale is large and comparable to the Planck mass.

When $\mu \sim M_{pl}$ according to (24) at large Λ^+ massive KK-modes can be produced in the interaction of UHECRs with atmosphere. However, in high energy accelerators this process can be observed only if the KK-mode interacts with another parton or the virtual photon with high transverse momentum. But in presence of many soft particles in the swarm, the probability of this type of events is very small. In an air-shower however the KK-mode does not need to have a large transverse momentum to be observed. Because of its mass (or in another word its propagation in the bulk) a delay should be observed as discussed in [1]. On the other hand, if μ is comparable to presumed electroweak scale $\sim TeV$, the main part of the swarm will be in the bulk and the delay they make in the air-shower can constraint the parameters of the model unless a symmetry - presumably related to quantum gravity - prevents the propagation to the bulk at the scale of UHECRs i.e. $\sim 10^{15} eV$. In the next section we discuss these arguments in a more quantitative way.

3 Gluon Distribution Function

Measurable quantities in hadron-hadron or hadron-lepton collisions which give the information about QCD interactions are parton distributions notably gluon distribution because of their dominance at high CM energy collisions. We define the gluon distribution function (structure function) in LC gauge [29] and 4+1 space-time as the following:

$$\begin{aligned} x_b G(x_b, Q^2, z) &= \frac{1}{(2\pi)^3} \int d^2k_\perp \Theta(Q^2 - k_\perp^2) \int dk^+ 2k^+ \delta(x_b - \frac{k^+}{P^+}) \\ &\int dy' e^{\mu y} \Big\langle \mathcal{A}^i(x^+, \vec{k}, y') \mathcal{A}_i(x^+, -\vec{k}, y - y') \Big\rangle \end{aligned} \tag{29}$$

$$\vec{k} = (k^+, k^\perp) \qquad z = \frac{1}{\mu} e^{\mu y} \quad , \quad i = x^\perp, z \tag{30}$$

where z is the bulk coordinate in metric (4), Q^2 is the 3-dim transverse momentum scale i.e. $x_b G(x_b, Q^2, z)$ is the density of soft/semi-soft gluons up to $|k_\perp| < Q$. The brackets $\langle\rangle$ indicate the average over all possible $\rho(\vec{x})$ (summation over spin and color is implicit). The reason for expressing the integral on y and not z is that y behaves as an additive coordinate and therefore the expression of correlations is simpler. The field $\mathcal{A}^i$ is the classical solution in MV approximation. This expression for gluon distribution is valid only in LC gauge. Rationale behind this definition has been explained in detail in [24] and [29] and here we briefly review the main points in the contest of 4+1 dimensional brane models.

In light-cone quantization, gluon field A^i in (7) can be expanded with respect to creation and annihilation operators:

$$A_a^B(x^+, x^-, x^\perp, z) = \sum_n \sum_\lambda \int \frac{d^3k}{\sqrt{(2\pi)^3 2k^+}} \Big[\epsilon_\lambda^B(z) u_n(z) e^{-ik.x} \alpha_{a\lambda}(\vec{k}, n) + \epsilon_\lambda^{*B}(z) u_n^*(z) e^{ik.x} \alpha_{a\lambda}^\dagger(\vec{k}, n) \Big] \tag{31}$$

Operators $\alpha_{a\lambda}$ and $\alpha_{a\lambda}^\dagger$ are respectively annihilation and creation operators and have usual commutation relation imposed by quantization. The index n indicates n^{th} KK-mode and $u_n(z)$ is the corresponding solution of the dynamic equation (10). Vector $\epsilon_\lambda^B(z)$ is 5-dim polarization vector. Due to non-flat geometry however it depends on z, but with the conformal form of the RS-metric, it can be easily related to the same quantity in local Lorentz frame [30]:

$$\epsilon_\lambda^B(z) = \frac{z}{R} \epsilon'^B_\lambda \tag{32}$$

where ϵ'^B_λ behaves like a vector in a flat 5-dimensional space-time. Gluon distribution is defined as expectation value of gluon number $< \psi | a^\dagger a | \psi > \propto < A^i A_i >$ where $|\psi>$ presents a color charge state (quarks), summed over allowed momentum, colors, polarization and KK-modes. After adding Wilson-line operator as explained in Sec.2.1, at classical level one can replace the quantum field A^i with the

classical solution $\mathcal{A}^i$ explained below. We should also sum over all quark states or equivalently add a probability distribution for charge sources. The final expression is equation (29).

Probability distribution of ρ - the functional $W(\rho)$ - can be only calculated in the quantum extension of the MV model. At classical level (which is enough when Λ^+ is large), we can assume a Gaussian distribution[4]. Therefore, the mean value of $\mathcal{O}(\rho)$ any functional of ρ can be calculated:

$$\langle \mathcal{O}(\rho) \rangle = \mathcal{N} \int \mathcal{D}\rho \exp\left\{ - \int d^4\vec{x} \frac{R^5}{z^5} \frac{tr(\rho(\vec{x}))^2}{2\sigma^2_{\Lambda^+}} \right\} \mathcal{O}(\rho) \tag{33}$$

$$\mathcal{N}^{-1} = \int \mathcal{D}\rho \exp\left\{ - \int d^4\vec{x} \frac{R^5}{z^5} \frac{tr(\rho(\vec{x}))^2}{2\sigma^2_{\Lambda^+}} \right\} \tag{34}$$

The function $\sigma^2_{\Lambda^+}$ which plays the rôle of standard deviation of the Gaussian distribution must be proportional to the total color charge density [25]:

$$\sigma^2_{\Lambda^+} \equiv \frac{g^2 n(\vec{x})}{2N_c} \tag{35}$$

where $n(\vec{x})$ is the color charge density with $\Lambda^+ = x_b P^+$ and N_c is the number of colors. Evidently we don't know the exact form of $n(\vec{x})$. Only in the quantum extension of the MVCGC model (see next section), one can determine the approximate Gaussian distribution and the functional form of $\sigma^2_{\Lambda^+}$. In general $\sigma^2_{\Lambda^+}$ depends on transverse coordinates including z. However, when $\Lambda^+ \gg \Lambda_{QCD}$, the color charge sheet is roughly infinite and σ_{Λ^+} will be roughly constant along transverse directions. Due to the warping however this argument does not apply to the extension to the bulk.

We don't have an explicit solution which directly relates $\mathcal{A}^i$ to ρ. But in the path integral (33) if we change the integration functional from ρ to $\tilde{A}^+$, the Jacobian of the transformation does not depend on ρ [28]. Using (15) and (16) the path integral (33) can be transferred to $\tilde{A}^+$ space:

$$\langle \mathcal{O}(\tilde{A}^+) \rangle = \mathcal{N} \int \mathcal{D}\tilde{A}^+ \exp\left\{ - \int d^4\vec{x} \frac{R^5}{z^5} \frac{tr(\partial_{;i}\partial^i_{;}\tilde{A}^+(\vec{x}))^2}{2\sigma^2_{\Lambda^+}} \right\} \mathcal{O}(\rho) \tag{36}$$

Following [24] analysis, we choose boundary condition for $\mathcal{A}^i$ as:

$$\mathcal{A}^i(x^- \to -\infty, x^\perp, z) \to 0 \tag{37}$$

which using (12) and (14)) leads to:

$$\mathcal{U}(x^- \to -\infty, x^\perp, z) \to cte. \qquad \tilde{A}^+(x^- \to -\infty, x^\perp, z) \to 0 \tag{38}$$

After fixing boundary values, equation (12) and properties of ordering operator [28] lead to:

$$\mathcal{A}^i(x^-, x^\perp, z) = \int_{-\infty}^{x^-} d\eta^- \mathcal{U}_{x_0^-=-\infty}(\eta^-, x^\perp, z) \partial^i_{;} \tilde{A}^+ \mathcal{U}^\dagger{}_{x_0^-=-\infty}(\eta^-, x^\perp, z) \tag{39}$$

Finally (39) can be used in (29) to calculate the gluon distribution. We expand $\mathcal{U}$ and $\mathcal{U}^\dagger$ with respect to power of g the coupling constant:

$$\mathcal{U}_{x_0^-=-\infty} = I - ig \int_{-\infty}^{x^-} d\eta^- \frac{R^2}{z^2} \tilde{A}^+(\eta^-, x^\perp, z) + \dots \tag{40}$$

At zero-order:

$$\begin{aligned} \left\langle \mathcal{A}^i_a(x^-, x^\perp, z) \mathcal{A}^j_b(x'^-, x'^\perp, z') \right\rangle_0 &\equiv \mathcal{N} \int \mathcal{D}\tilde{A}^+ \Bigg[\exp\left\{ - \int d^4\vec{x}'' \frac{R^5}{z''^5} \frac{tr(\partial_{;k}\partial^k_{;}\tilde{A}^+(\vec{x''}))^2}{2\sigma^2_{\Lambda^+}} \right\} \\ &\int_{-\infty}^{x^-} d\eta^- \frac{R^2}{z^2} \partial^i_{;} \tilde{A}^+_a(\eta^-, x^\perp, z) \int_{-\infty}^{x^-} d\eta'^- \frac{R^2}{z'^2} \partial^j_{;} \tilde{A}^+_b(\eta'^-, x'^\perp, z') \Bigg] \\ &= \delta_{ab} \chi \partial^i_{;} \partial'^j_{;} \frac{1}{(\partial_{;k}\partial'^k_{;})^2}(x^\perp, z, x'^\perp, z') \end{aligned} \tag{41}$$

[4]Simulations show that Gaussian assumption for fragmentation is a good approximation at UHECR energy scale [31].

$$\chi \equiv \frac{(zz')^{\frac{1}{2}}}{R}\int_{-\infty}^{max(x^-,x'^-)} dx''^- \sigma_{\Lambda^+}(x''^-,x^\perp,z)\sigma_{\Lambda^+}(x''^-,x'^\perp,z') \tag{42}$$

The inverse of operator $(\partial_{;k}\partial^k_{;})^{-2}$ can be defined using equation (20) and its solution (23):

$$\begin{aligned}(\partial_{;k}\partial'^k_{;})^{-2}\delta^3(x^\perp - x'^\perp,z,z') \quad &\equiv \quad \gamma(x^\perp,x'^\perp,z,z') = \frac{1}{(2\pi)^2}\int_{\Lambda_{QCD}} d^2k\perp e^{-ik_\perp(x^\perp - x'^\perp)} \\ &\int_R^{R'} \frac{dz''}{R^4}\Delta(z'',z,k^\perp)\Delta(z'',z',k^\perp) + \gamma(0)\end{aligned} \tag{43}$$

The constant term $\gamma(0)$ includes singularities of the operator [28]. We have also taken into account the QCD infrared cutoff Λ_{QCD}.

In the same way one can calculate terms proportional to higher orders of g. Finally, at classical level the matrix element $\langle \mathcal{A}^i_a \mathcal{A}^j_b\rangle$ is:

$$\begin{aligned}\left\langle \mathcal{A}^i_a(x^-,x^\perp,z)\mathcal{A}^j_b(x'^-,x'^\perp,z')\right\rangle \quad &= \quad -\delta_{ab}\left(\partial^i_{;}\partial'^j_{;}\gamma(x^\perp,x'^\perp,z,z')\right)\frac{1}{\gamma(x^\perp,x'^\perp,z,z')-\gamma(0)} \\ &\left(1-\exp\left\{\chi(\vec{x},\vec{x'},z,z')\left(\gamma(x^\perp,x'^\perp,z,z')-\gamma(0)\right)\right\}\right)\end{aligned} \tag{44}$$

The interesting point about this result is that dependence on x^- is only through the unknown charge distribution which appears as a coefficient of the exponential and the rest can be calculated analytically.

Integrals in momentum space of the right hand side of (29) can be changed to real space using inverse Fourier transform:

$$x_bG(x_b,Q^2,z) = 2J_1(1)P^+x_bQ^2\int d^3\vec{x}e^{iP^+x_bx^-}x^{\perp 2}\int d^3\vec{x'}\int_0^L dy'e^{\mu y'}\left\langle \mathcal{A}^i(x^+,\vec{x'},y')\mathcal{A}_i(x^+,\vec{x}-\vec{x'},y-y')\right\rangle \tag{45}$$

Therefore to calculate gluon distribution we can replace $\langle \mathcal{A}^i_a\mathcal{A}^j_b\rangle$ with (44). However, the expression would be very complex. When the exponent of the exponential term in (44) is small, one can expand this term. In fact it is the case because according to (35) χ depends on the coupling g^2. The expansion of the exponential in (44) corresponds to expansion with respect to the perturbative coupling. One can however argument that although g^2 can be small, the charge density χ can be very large and makes the exponent large. This happens specially at relatively low Λ^+ where the Gaussian approximation we have used here is not anymore valid. When this approximation applies i.e. for large Λ^+, the expression of $\langle \mathcal{A}^i_a\mathcal{A}^j_b\rangle$ at first order is very simple:

$$\left\langle \mathcal{A}^i_a(\vec{x},z)\mathcal{A}_{bi}(\vec{x'},z')\right\rangle = \delta_{ab}\chi(\vec{x},\vec{x'},z,z')\partial^i_{;}\partial'_{;i}\gamma(x^\perp,x'^\perp,z,z') + \dots \tag{46}$$

Using (43), (23) and explicit expression of the integration coefficient in (23) from Paper I, we can explicitly calculate $\langle \mathcal{A}^i\mathcal{A}_i\rangle$. In Sec.4.1 with numerical calculation of integrals in (43) we show that at least for small $k^2_\perp$ which have the largest amplitude, the integral over z'' in (43) does not strongly depend on the transverse momentum. Therefore in (46), the correlation integral reflects the distribution of gluons in the bulk and we expect that after performing integrals over the rest of the spatial coordinates, the z dependence of gluon distribution can not be significantly different. By contrast gluon distribution strongly depends on the distribution of color charge $\chi(\vec{x},\vec{x'},z,z')$ which in this classical approximation level is unknown. It is easy to see that only if σ_{Λ^+} does not have any extension in the bulk i.e. $\sigma_{\Lambda^+}\propto\delta(z-R')$, gluons are confined to the visible brane. As we have discussed before such a distribution is inconsistent.

In [20] the condition for quasi-confinement of vector fields is the confinement of charges (here color charges) to the brane. MV-model shows that in the case of QCD, due to relatively strong self-interaction of gluons (even in perturbative regime), if gluons propagate into the bulk, many quarks follow them because valance quarks have a small contribution in the total density of quarks and the strategy of charge confinement will fail.

4 Quantum extension of MVCGC Model

Classical MV model is applicable to high momentum scales when the rapidity $\tau \equiv \ln(1/x_b)$ is small (i.e. closer to the color charge sheet) and the density of partons (gluons) $\propto \alpha_s \tau$ is small and tree level (classical) approximation is adequate. This regime also corresponds to the high energy scale in which physics is presumably higher dimensional. This classical approximation however leaves some important quantities like $W[\rho]$ undetermined. Even when the Gaussian approximation discussed in the previous section the standard deviation σ_{Λ^+} or equivalently χ in (42) is undetermined and therefore it is not possible to estimate the distribution of gluons.

A more quantitative insight to the processes and cross-sections is achievable when the action which leads to equation (7) - the classical field equation in LC gauge - is quantized by a path integral method in presence of a charge ρ:[5]

$$\mathcal{Z}[j] = \int \mathcal{D}\rho W_{\Lambda^+}[\rho] \left\{ \frac{\int^{\Lambda^+} \mathcal{D}A\delta(A^+) e^{iS[A,\rho] - \int d^5x\sqrt{-g}A.j}}{\int^{\Lambda^+} \mathcal{D}A\delta(A^+) e^{iS[A,\rho]}} \right\} \tag{47}$$

Evaluation of quantum corrections to the classical solution is performed by determining quantum perturbations around classical solution due to an infinitesimal change of the scale Λ^+. The classical solution $\mathcal{A}^B$ is therefore replaced by:

$$A^B(x^+, \vec{x}, z) = \mathcal{A}^B(x^+, \vec{x}, z) + \delta A^B(x^+, \vec{x}, z) + a^B(x^+, \vec{x}, z) \tag{48}$$

where δA^B presents perturbation of soft gluon contribution to $\mathcal{A}^B$ due to scale change and a^B is semi-hard interactions contribution. In fact when Λ^+ is scaled down to $b\Lambda^+$ with $0 < b < 1$, partons with momentum $b\Lambda^+ < |k| < \Lambda^+$ are not anymore summed into soft gluon swarm. Because the main assumption of MVCGC is that at each scale the classical field equation (7) with random charge ρ determines the distribution of gluons, a change in the scale must be similar to a change in the charge. In other word a small modification of longitudinal momentum scale Λ^+ is equivalent to a small modification of the charge distribution $\rho \to \rho + \delta\rho$. Using this equivalence, one finds a functional differential equation similar to renormalization group equation [25]:

$$\frac{\delta W_\tau[\rho]}{\delta\tau} = \alpha_s \left\{ \frac{1}{2} \frac{\delta^2}{\delta\rho^a_\tau(x^\perp, z)\delta\rho^b_\tau(x'^\perp, z')} [W_\tau \chi^{ab}] - \frac{\delta}{\delta\rho^a_\tau(x^\perp, z)} [W_\tau \sigma^a] \right\} \tag{49}$$

where $\tau = \ln(P^+/\Lambda^+)$. Indexes a and b are color index in the same representation as gluons (i.e. in conjugate representation). Matrix elements σ^a and χ^{ab} are defined as:

$$\sigma^a = \langle \delta\rho^a \rangle \tag{50}$$

$$\chi^{ab} = \langle \delta\rho^a \delta\rho^b \rangle \tag{51}$$

As usual $\langle\rangle$ means average over all values of ρ i.e. J^+ component of the color current J^B. Lowest order QCD diagrams which contribute to charge variation are discussed in [25].

In Gaussian approximation $T_{ab}\chi^{ab} \sim \sigma^2_{\Lambda^+}$ defined in (35). At lowest order (BFKL approximation) [25]:

$$\sigma^a \approx -g^2 D^+_y Tr\left(T^a G^i_{0i}(x, y) \right)\Big|_{x=y} \tag{52}$$

$$\chi_{ab} \approx 4ig^2 \mathcal{F}^{+i}_{ac}(x) \langle x|G_{0ij}|y\rangle \mathcal{F}^{+j}_{cb}(y) \tag{53}$$

$$G_0^{ij\,-1}(x) = g^{ij}\partial_{;B}\partial^B_{;} \quad , \quad i = \perp, z \tag{54}$$

[5]The charge source ρ is not really an independent source because it is produced by gluons [25]. Therefore the path integral over the functional ρ is similar to a condition or a subset of possible solutions rather than summing over possible values of an external source. For this reason the functional integral over ρ is applied after determining the expectation value of an arbitrary operator.

where G_0^{ij} is the propagator of free gluons. Its z dependence is similar to γ defined in (43). In equation (53) $\mathcal{F}_{ac}^{+i}$ is the gluon field strength of classical solution (39). This approximation evaluation of χ can be used in (46) to determine the gluon distribution up to BFKL approximation. Due to complexity of $T^{ab}\chi_{ab}$ and the fact that we are only interested in z dependence of $\sigma^2_{\Lambda^+}$ (or more exactly χ defined in (42)), we try to find the dominant z dependent term in $T^{ab}\chi_{ab}$.

Considering various components which contribute to (53), one finds that up to a factor depending only on Bessel functions:

$$T^{ab}\chi_{ab} \sim \sigma^2_{\Lambda^+} \propto \left(\frac{zz'}{R^2}\right)^n \qquad n \sim \frac{3}{2} \tag{55}$$

This is estimated by the following arguments: From (39) and (40) at zero-order in coupling g (i.e. free gluons):

$$\mathcal{A}^i \sim \int d\vec{x'}\rho(\vec{x'}) \int_{-\infty}^{x^-} d\eta^- \partial^i_{;} \Delta(\eta^-, x^\perp, z, \vec{x'}) \tag{56}$$

Therefore:

$$\begin{aligned} \mathcal{F}^{i+}(x) = -\partial^+_{;}\mathcal{A}^i \quad \sim \quad & \int d\vec{x'}\rho(x') \Bigg[g^{+-} g^{ij} \partial_- \left(\int_{-\infty}^{x^-} d\eta^- \partial_{;j} \Delta(\eta^-, x^\perp, z, \vec{x'}) \right) - z g^{+-} \delta^{i\perp} \\ & \int_{-\infty}^{x^-} d\eta^- \partial_{;5} \Delta(\eta^-, x^\perp, z, \vec{x'}) + 2z g^{+-} \delta^{i5} \int_{-\infty}^{x^-} d\eta^- \partial_{;\perp} \Delta(\eta^-, x^\perp, z, \vec{x'}) \Bigg] \end{aligned} \tag{57}$$

Applying (57) into (53) and using (52) as the average value of ρ in (57) as well as the expression for $\Delta(z, z')$ (23), one finds (55).

BFKL approximation is valid when the density of partons is not very high i.e. at large Λ^+ scale. The renormalization group equation (49) can be used to obtain W at lower scales, up to approximation order in which σ^a and χ^{ab} are calculated. An analytical solution of equation (49) however is not available even for the simpler case of a flat 4-dim space-time. Nevertheless, some qualitative aspects of the solution at high energy scales can be used to estimate the properties of the gluon distribution at lower energies specially in what concerns their propagation into the bulk. For instance z-dependence of σ^a and χ^{ab} in (52) and (55) as well as numerical calculation of the next section is an evidence for emission of a large amount of partons in the bulk at lower scales because their parent partons at high energy scales are in the bulk and although they have lower energies, they are yet highly relativistic and can overcome the gravitational bending (see Paper I). The observational consequence is an abrupt reduction in the total DIS or hadron-hadron cross-section in colliders, assuming that a symmetry broken at scales smaller than Λ_{sb} prevents the propagation of partons in the bulk. As for UHECRs, a cutoff in their spectrum or at least a time decoherence is expected if after hadronization of partons, particles are pushed back by the warped metric to the visible brane. Such a cutoff or decoherence has not yet been observed either in colliders or in the flux of UHECRs up to CM energies of the order of $\sim 10^{15} eV$.

4.1 Numerical Calculation and Discussion

In this section we apply BFKL approximation for σ_{Λ_+} to equations (45) and (46) to determine $x_b G(x_b, Q^2, z)$ - the distribution of gluons in the bulk. As we have only an approximation for $\sigma^2_{\Lambda^+}$, to see how much a different z dependence in (55) can influence our conclusions, we also try a few other exponents in (55). Similar to Sec.3, we only focus on the dependence on bulk coordinate z. We study two sets of models: fine-tuned Randall-Sundrum models and models with $\mu = M_5 \gtrsim TeV$. In both cases we also modify the value of μL to see the effect of the bulk size.

Figures 1 and 2 show the distribution of gluons in the bulk normalized to its value on the visible brane i.e. the brane at $z = R'$ for respectively fine-tuned Randall-Sundrum models and models with a compactification scale similar to fundamental gravitation scale M_5. In the first case the size of the bulk

is macroscopic and according to this approximate model, gluons are distributed roughly uniformly in the bulk with a couple of orders of magnitude increase on the hidden brane due to larger coupling of KK-modes (see (27) and (28)). When the bulk is small, gluons have tendency to accumulate strongly on the hidden brane where the coupling is larger. The dependence on $k_\perp$ in this case is quite regular and decreases with increasing M_5.

In Dvali *et al.* [13] induced coupling method for semi-confinement of vector fields, the compactification scale is related to coupling constants $p^* = 2g^{*2}/g^2$ where p^* is the compactification scale and g^{*2} is the induced coupling on the visible brane. The scale p^* must be very small to be compatible with observations. According to results shown in Fig.1 however, even in a warped geometry which partially confines all the fields and up to scales as small as $10^{-17}eV$, gluons propagate into the bulk and the additional coupling can not stop them. In fact, if the origin of induced coupling is the renormalization terms which must be added to the bare Lagrangian due to presence of branes, one expects that $g^{*2}\nu/g^2 \sim \mathcal{O}(1)$ where ν is related to the size of the bulk, $\nu \to 0$ when the distance between branes approaches infinity. This adds terms proportional to a 4-dim. delta function to (9) as well as to (52) and (53). These additional terms must be proportional to ν and approach to zero when the distance between branes becomes large. Therefore, one expects that the induced charge increases the amplitude of gluon distribution on the visible brane by a factor proportional to $g^{*2}\nu/g^2 \sim \mathcal{O}(1)$ which is not very efficient when the probability of finding gluons in the bulk is orders of magnitude larger.

To see the effect of n - the power of zz'/R^2 in (55) - Fig.3 compares the simulation for 3 different value of n. It shows that with decreasing n gluons concentrate more on hidden brane. A larger power moves the concentration toward visible brane, but even with a power as large as 3, the distribution in the bulk and on the branes is roughly uniform. Therefore only an unlikely $n \gg 3$ can concentrate gluons on the visible brane.

Direct comparison of these results with what has been obtained in Paper I with classical treatment of propagation is difficult. The first reason is that here we studied non-hadronized partons. When particles propagate in the bulk and hadronize, their coupling changes and consequently their propagation will not be the same. This is important for models with macroscopic bulk like RS fine-tuned model, but irrelevant when the bulk size is smaller than Λ_{QCD}^{-1}. Therefore one should not make strong conclusions from what is shown in Fig.1, although it is not completely irrelevant either. This figure shows the behavior of a vector field with MVCGC phenomenological Lagrangian. Although the distribution of partons depends on the integration along the bulk, at short distances from the visible brane the distribution should not be very different, specially in what concerns the escape of partons to the bulk. We make this conclusion based on the results shown in Fig.2 for microscopic bulk. Eventually, one can limit the integral in (43) to $R_{QCD} \equiv R\exp(\mu/\Lambda_{QCD})$ and for the rest of the path one can use a free propagator. As our purpose here is demonstration of principals, we don't go through these details.

In summary, we have shown that the effect of an extra-dimension is not limited to the high transverse momentum interactions. It affects all intermediate steps and thereby the total cross-section of interactions. In hadron-hadron and hadron-lepton colliders where most energetic parts of the remnants are lost in the detector hole, the effect should appear as a cutoff in the total cross-section at high energies and a reduction in the final multiplicity of events. The same cutoff should be also observable in air-showers and/or a time decoherence in the shower must be detectable due to different propagation time in the bulk. Identification of a cutoff as being due to extra-dimension is however less evident because whatever the source of UHECRs - top-down or acceleration in astronomical sources - one expects a cutoff at high energy part of the spectrum.

The method used in this work has the advantage to be more exact in treating microscopic physics of the interaction of high energy particles and the influence of an extra-dimension on them. It is however more complex and its application to more complicated brane models is difficult. The classical treatment of Paper I by contrast is simpler and can be used to find a rough estimation of acceptable range of parameters for a given brane model.

References

[1] Ziaeepour H., *"Testing Brane World Models with Ultra High Energy Cosmic Rays"*, hep-ph/0203165.

[2] Antoniadis I., *Phys. Lett.* B **246**, (1990) 377, Horava P. & Witten E., *Nucl. Phys.* B **460**, (1996) 506 hep-th/9510209, Horava P. & Witten E., *Nucl. Phys.* B **475**, (1996) 94 hep-th/9603142.

[3] Arkani-Hamed N., Dimopoulos S. & Dvali G., *Phys. Lett.* B **429**, (1998) 263 hep-ph/9807344; Antoniadis I., *et al.*, *Phys. Lett.* B **436**, (1998) 257 hep-ph/9804398.

[4] Randall L. & Sundrum R., *Phys. Rev. Lett.* **83**, (1999) 3370 hep-ph/9905221, Randall L. & Sundrum R., *Phys. Rev. Lett.* **83**, (1999) 4690 hep-ph/9906064.

[5] Dimopoulos S. & Giudice G.F., *Phys. Lett.* B **379**, (1996) 105, Long J.C., Chan H.W. & Price J.C., *Nucl. Phys.* B **539**, (1999) 23 hep-ph/9805217.

[6] Arkani-Hamed N., Dimopoulos S. & Dvali G, PLB **429**, (1998) 263 hep-ph/9807344, Fairbairn M. & Griffiths L.M., *J. High Ener. Phys.* **0202**, (2002) 024 hep-ph/0111435.

[7] Davis A.Ch., Rhodes Ch. & Vernon I., *J. High Ener. Phys.* **0111**, (2001) 015 hep-ph/0107250, Brax Ph. & Davis A.C., hep-th/0104023, Davis S.C. *J. High Ener. Phys.* **0203**, (2002) 058 hep-ph/0111351

[8] Giudice G.F., Rattazzi R., & Wells J.D., *Nucl. Phys.* B **544**, (1999) 3 hep-ph/9811291, Hall L.J. & Smith D., *Phys. Rev.* D **60**, (1999) 085008 hep-ph/9904267.

[9] Davoudiasl H., Hewett J.L. & Rizzo T.G. *Phys. Rev.* D **63**, (2001) 075004 hep-ph/0006041.

[10] Fairbairm M. & Griffiths L.M. *J. High Ener. Phys.* **0202**, (2002) 024 hep-ph/0111435.

[11] Ziaeepour H., *"Two-Brane Models and BBN"* hep-ph/0010180.

[12] Anchordoqui L.A., Feng J.L., Goldberg H. & Shapere A.D. *Phys. Rev.* D **65**, (2002) 124027 hep-ph/0112247.

[13] Dvali G., Gabadadze G. & Shifman M., *Phys. Lett.* B **497**, (2001) 271 hep-th/0010071.

[14] Dubovsky S.L., Rubakov V.A., *Int. J. Mod. Phys.* A **16**, (2001) 4331 hep-th/0105243.

[15] Dubovsky S.L., Rubakov V.A. & Tinyakov P.G., *Phys. Rev. Lett.* **85**, (2000) 3769 hep-ph/0006046, Dubovsky S.L., Rubakov V.A. & Tinyakov P.G., *J. High Ener. Phys.* **0008**, (2000) 041 hep-ph/0007179.

[16] Davoudiasl H., Hewett J.L. & Rizzo T.G., *Phys. Lett.* B **473**, (2000) 43 hep-ph/9911262, Davoudiasl H., Hewett J.L. & Rizzo T.G., *Phys. Rev.* D **68**, (2003) 045002 hep-ph/0212279, Davoudiasl H., Hewett J.L. & Rizzo T.G., *J. High Ener. Phys.* **0308**, (2003) 034 hep-ph/0305086.

[17] Giddings S.B., Katz E. & Randall L., *J. High Ener. Phys.* **0003**, (2000) 023 hep-th/0002091.

[18] Bajc B. & Gabadadze G.,*Phys. Lett.* B **474**, (2000) 282 hep-th/9912232.

[19] Dubovsky S.L. *J. High Ener. Phys.* **0201**, (2002) 012 hep-th/0103205.

[20] Dvali G., Gabadadze G. & Porrati M., *Phys. Lett.* B **484**, (2000) 112 hep-th/0002190, Dvali G., Gabadadze G. & Porrati M.,*Phys. Lett.* B **484**, (2000) 129 hep-th/0003054.

[21] Carena M., Tait T.M.P., & Wagner C.E.M., hep-ph/0207056.

[22] Oda I., hep-th/0103257.

[23] Gogberashvili M. & Singleton D., *Phys. Rev.* D **69**, (2004) 026004 hep-th/0305241.

[24] McLerran L. & Venugopalan R., *Phys. Rev.* D **49**, (1994) 2233, McLerran L. & Venugopalan R., *Phys. Rev.* D **49**, (1994) 3352, McLerran L. & Venugopalan R., *Phys. Rev.* D **50**, (1994) 2225.

[25] Iancu E., Leonidov A., & McLerran L., hep-ph/0011241, Ferreiro E., Iancu E., Leonidov A., & McLerran L., hep-ph/0109115.

[26] Anderson B. *et al.*(The small x Collaboration) hep-ph/0204115.

[27] McLerran L., *"What is the Evidence for Color Glass Condensate"*, hep-ph/0402137.

[28] Jalalian-Marian J., *et al.*, *Phys. Rev.* D **55**, (1997) 5414 hep-ph/9606337.

[29] Mueller A.H., hep-ph/9911289.

[30] Birrell N.D. & Davies P., "Quntum field in curved space", Cambridge University Press, 1999.

[31] Basu R. & Bhattacharjee P., peh-ph/0403299.

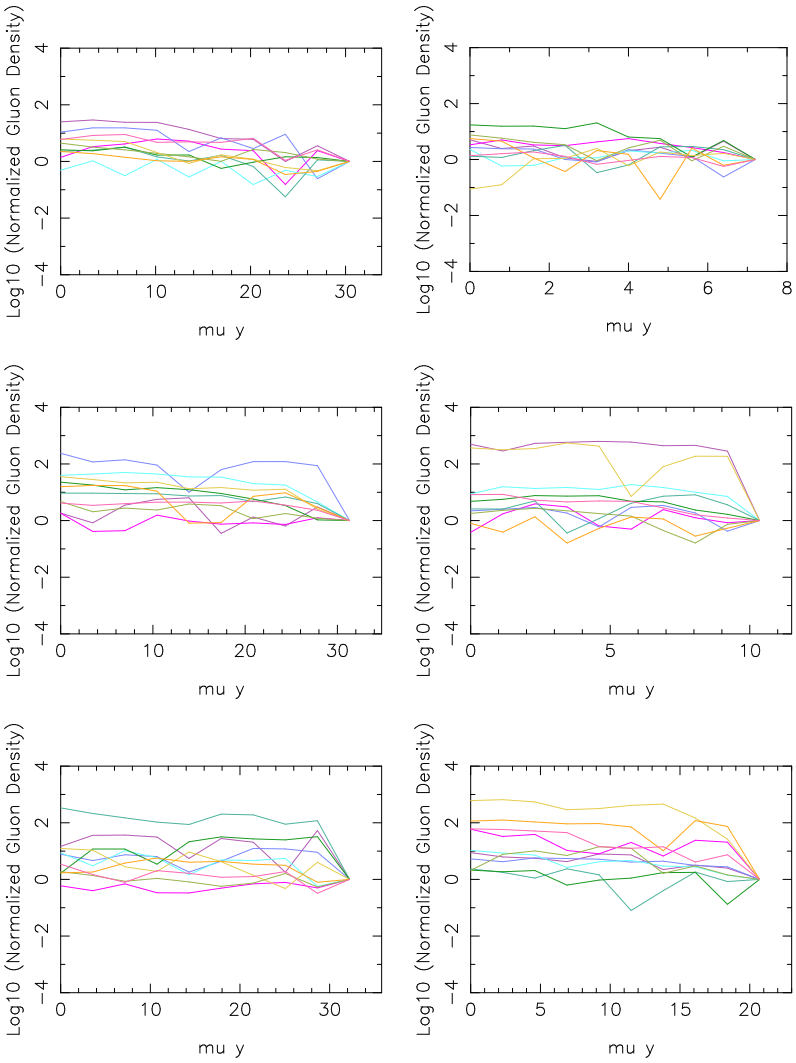

Figure 1: Gluon distribution in the bulk normalized to the amplitude of the distribution on the visible brane at $z = R'$ for Randall-Sundrum models for $2 \times 10^8 eV \leqslant |k_\perp| \leqslant 1.26 \times 10^{10} eV$. Curves are rainbow color coded. From bottom to top $M_5 = 10^{13} eV, 10^{14} eV$ and $10^{15} eV$, with μ obtained from fine-tuned RS model (3) i.e. $\mu = 10^{-17} eV, 10^{-14} eV$ and $10^{-11} eV$ respectively. For left plots $\log(R'/R) = \log(M_{pl}/M_5)$, i.e. the same as (2). In right panel a smaller R'/R is used to see the effect of a smaller bulk with same fundamental gravitation and compactification scale. Our tests show that apparent vibration of the distribution is mainly due to low resolution of our numerical calculation.

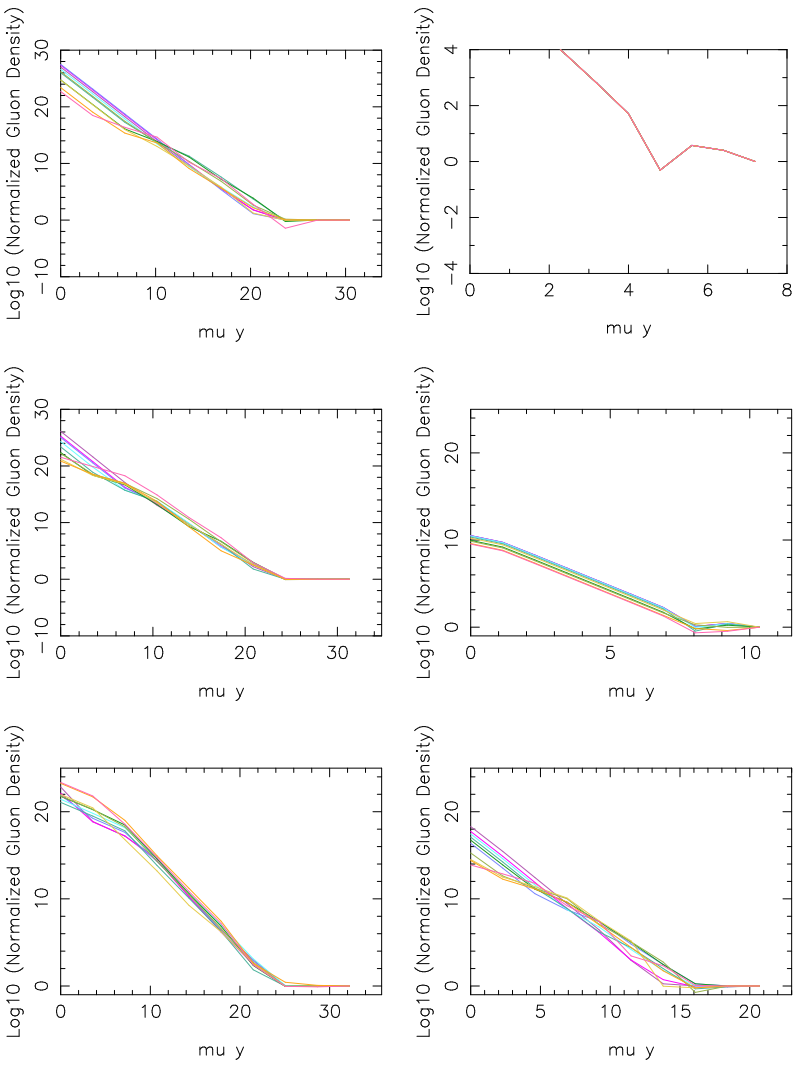

Figure 2: The same as Fig.1 but with $\mu = M_5$. Other details are the same as Fig.1. In the top right plot the difference between curves for different $k^{\perp}$ is much smaller than the resolution of this figure and they are overlapped.

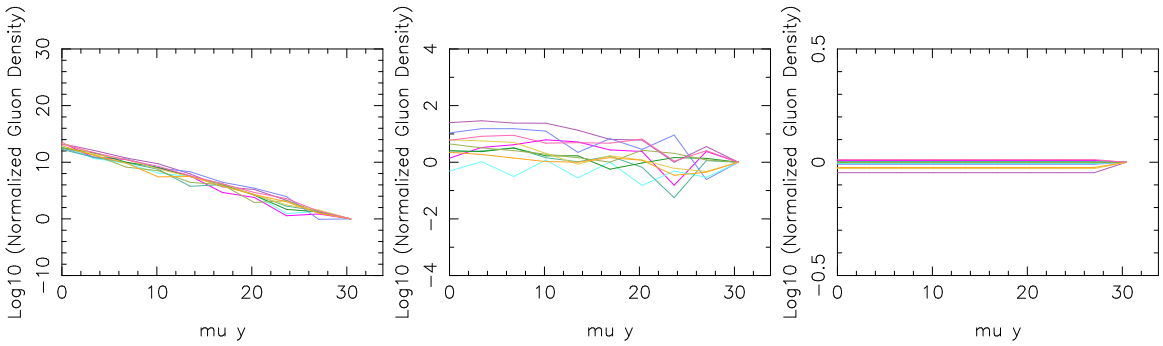

Figure 3: Distribution of gluons in fine-tuned RS models with $M_5 = 10^{15} eV$ for three values of n in (55). From left to right: $n = 1, 3/2$ (our estimation from BFKL approximation) and 3. Other details are the same as Fig.1.